*Epilepsia*, **48**(9):1774–1784, 2007
Blackwell Publishing, Inc.


# Pharmacoresistance in Epilepsy: A Pilot PET Study with the P-Glycoprotein Substrate *R*-[$^{11}$C]verapamil

*†Oliver Langer, *Martin Bauer, ‡§Alexander Hammers, ¶Rudolf Karch, ‖Ekaterina Pataraia, §Matthias J. Koepp, *Aiman Abrahim, **Gert Luurtsema, *Martin Brunner, ††Raute Sunder-Plassmann, ‖Friedrich Zimprich, *Christian Joukhadar, ‡‡Stephan Gentzsch, §§Robert Dudczak, §§Kurt Kletter, *Markus Müller, and ‖Christoph Baumgartner

**Department of Clinical Pharmacology, Division of Clinical Pharmacokinetics, Medical University of Vienna, Vienna, Austria; †Department of Radiopharmaceuticals, Austrian Research Centers GmbH – ARC, Seibersdorf, Austria; ‡Division of Neuroscience, Faculty of Medicine, Imperial College, and MRC Clinical Sciences Centre, Hammersmith Hospital, London, UK; §Department of Clinical and Experimental Epilepsy, Institute of Neurology, University College London, United Kingdom; ¶ Department of Medical Computer Sciences, Medical University of Vienna, Vienna, Austria; ‖Department of Neurology, Medical University of Vienna, Vienna, Austria; **Department of Nuclear Medicine & PET Research, VU University Medical Center, Amsterdam, The Netherlands; ††Institute of Medical and Chemical Laboratory Diagnostics, Medical University of Vienna, Vienna, Austria; ‡‡Department of Radiology, Division of Neuroradiology, Medical University of Vienna, Vienna, Austria; and §§Department of Nuclear Medicine, Medical University of Vienna, Vienna, Austria*

**Summary:** *Purpose and Methods:* Regional overexpression of the multidrug transporter P-glycoprotein (P-gp) in epileptic brain tissue may lower target site concentrations of antiepileptic drugs and thus contribute to pharmacoresistance in epilepsy. We used the P-gp substrate *R*-[$^{11}$C]verapamil and positron emission tomography (PET) to test for differences in P-gp activity between epileptogenic and nonepileptogenic brain regions of patients with drug-resistant unilateral temporal lobe epilepsy (n = 7). We compared *R*-[$^{11}$C]verapamil kinetics in homologous brain volumes of interest (VOIs) located ipsilateral and contralateral to the seizure focus. *Results:* Among different VOIs, radioactivity was highest in the choroid plexus. The hippocampal VOI could not be used for data analysis because it was contaminated by spill-in of radioactivity from the adjacent choroid plexus. In several other temporal lobe regions that are known to be involved in seizure generation and propagation ipsilateral influx rate constants $K_1$ and efflux rate constants $k_2$ of *R*-[$^{11}$C]verapamil were descriptively increased as compared to the contralateral side. Parameter asymmetries were most prominent in parahippocampal and ambient gyrus ($K_1$, range: −3.8% to +22.3%; $k_2$, range: −2.3% to +43.9%), amygdala ($K_1$, range: −20.6% to +31.3%; $k_2$, range: −18.0% to +38.9%), medial anterior temporal lobe ($K_1$, range: −8.3% to +14.5%; $k_2$, range: −14.5% to +31.0%) and lateral anterior temporal lobe ($K_1$, range: −20.7% to +16.8%; $k_2$, range: −24.4% to +22.6%). In contrast to temporal lobe VOIs, asymmetries were minimal in a region presumably not involved in epileptogenesis located outside the temporal lobe (superior parietal gyrus, $K_1$, range: −3.7% to +4.5%; $k_2$, range: −4.2% to +5.8%). In 5 of 7 patients, ipsilateral efflux ($k_2$) increases were more pronounced than ipsilateral influx ($K_1$) increases, which resulted in ipsilateral reductions (10%–26%) of *R*-[$^{11}$C]verapamil distribution volumes (DV). However, for none of the examined brain regions, any of the differences in $K_1$, $k_2$ and *DV* between the epileptogenic and the nonepileptogenic hemisphere reached statistical significance ($p > 0.05$, Wilcoxon matched pairs test). *Conclusions:* Even though we failed to detect statistically significant differences in *R*-[$^{11}$C]verapamil model parameters between epileptogenic and nonepileptogenic brain regions, it cannot be excluded from our pilot data in a small sample size of patients that regionally enhanced P-gp activity might contribute to drug resistance in some patients with temporal lobe epilepsy.
**Key Words:** Antiepileptic drugs—Pharmacoresistance—Temporal lobe epilepsy–P-glycoprotein—Positron emission tomography—*R*-[$^{11}$C]verapamil.

About one-third of patients suffering from epilepsy do not respond to treatment with antiepileptic drugs (AEDs). Pharmacoresistant epilepsy is characterized by a lack of treatment response to several different AEDs, despite the fact that these drugs possess different modes of action. This observation argues against the concept that treatment failure is solely associated with an alteration of molecular AED targets and rather points to the

Accepted February 13, 2007.
Markus Müller and Christoph Baumgartner had equal responsibility for this study.
Address correspondence and reprint requests to Dr. Oliver Langer, Department of Clinical Pharmacology, Division of Clinical Pharmacokinetics, Medical University of Vienna, Währinger-Gürtel 18–20, 1090 Vienna, Austria. E-mail: oliver.langer@meduniwien.ac.at
doi: 10.1111/j.1528-1167.2007.01116.x

involvement of other nonspecific mechanisms (Löscher and Potschka, 2002, 2005; Remy and Beck, 2006). Increasing evidence from immunohistochemical or mRNA analysis of brain tissue specimens removed during surgery of patients with pharmacoresistant epilepsy suggests that multidrug transporters, in particular P-glycoprotein (P-gp) and members of the multidrug resistance-associated proteins (MRP), are overexpressed in capillary endothelial cells and astrocytes of epileptogenic brain tissue (Tishler et al., 1995; Sisodiya et al., 1999; Dombrowski et al., 2001; Aronica et al., 2004). These active transporter proteins, which belong to the family of the ATP-binding cassette (ABC) transporters, are believed to contribute to the blood–brain barrier (BBB) by extruding a variety of lipophilic drugs from brain parenchyma including AEDs. Overexpression of P-gp and MRP in epileptogenic brain tissue might thus lower AED target site concentrations below effective levels and account for treatment refractoriness.

Due to limited access to brain tissue in vivo, only a small number of techniques is available to assess transporter function in the human brain. Results from microdialysis experiments in animal models suggest that several major AEDs (except for levetiracetam and valproic acid) are substrates of P-gp and/or MRP2 (Potschka and Löscher, 2001; Potschka et al., 2001, 2003, 2004; Baltes et al., 2006). Even though microdialysis for measurement of local brain AED concentrations in human epileptic brain tissue is feasible, ethical and methodological issues limit the use beyond experimental protocols (Rambeck et al., 2006).

An alternative approach to assess the function of multidrug transporters in the human brain in vivo is positron emission tomography (PET) with radiolabeled transporter substrates. To date, the best validated PET tracer for P-gp is the carbon-11-labeled calcium channel inhibitor [$^{11}$C]verapamil. At low (picomolar) concentrations, as given during PET experiments, verapamil has been shown to be effectively transported by P-gp at the BBB (Hendrikse et al., 1998; Sasongko et al., 2005; Syvänen et al., 2006a; Lee et al., 2006). Whereas initially developed as a racemic mixture (Elsinga et al., 1996), the use of enantiomerically pure *R*-[$^{11}$C]verapamil has recently been proposed for human PET studies (Lubberink et al., 2006). Even though both *R*- and *S*-verapamil are substrates for P-gp (and not for MRP), differences in metabolism and plasma protein binding of the two enantiomers suggest that an enantiomerically pure radiotracer would be preferable for the kinetic modeling of PET data (Franssen et al., 2006; Lubberink et al., 2006).

[$^{11}$C]Verapamil has been used in several human PET studies both in young and elderly healthy volunteers (Brunner et al., 2005; Sasongko et al., 2005; Toornvliet et al., 2006) and in Parkinson patients (Kortekaas et al., 2005). Regional increases in the DV of the radiotracer in patients were suggestive of impairment of the BBB.

In the present pilot study, we used *R*-[$^{11}$C]verapamil PET in patients with medically refractory temporal lobe epilepsy (TLE) in order to test for potential differences in P-gp activity between epileptogenic and nonepileptogenic brain regions. We hypothesized that overexpression of P-gp would lead to increased efflux and reduction of *DV* of the radiotracer.

## Methods

The study protocol was approved by the local Ethics Committee and was performed in accordance with the Declaration of Helsinki (1964) in the revised version of 2000 (Edinburgh), the Guidelines of the International Conference of Harmonization, the Good Clinical Practice Guidelines and the Austrian drug law (Arzneimittelgesetz). All subjects were given a detailed description of the study and their written consent was obtained prior to the enrollment in the study.

### Patients

We studied seven patients (two women) suffering from medically refractory TLE, who underwent presurgical evaluation at our center. Patient characteristics are shown in Table 1. The diagnosis and focus lateralization was based on clinical seizure semiology, interictal electroencephalography (EEG) abnormalities, ictal EEG findings and detailed neuropsychological assessment. Six patients had unilateral hippocampal sclerosis concordant with the side of the seizure focus and one patient had a normal MRI. All patients fulfilled criteria of medical intractability (Bourgeois, 2001). The mean age at onset of habitual seizures was 16 years (range 3–36 years), the mean duration of epilepsy before the PET examination was 30 years (range 13–51 years) and the mean age at PET examination was 46 years (range 33–54 years). All patients were genotyped for *ABCB1* single nucleotide polymorphisms (SNPs) in exons 12 (C1236T), 21 (G2677T) and 26 (C3435T) by employing previously described procedures (Sunder-Plassmann et al., 2005) (Table 1).

### PET experimental procedure

PET images were acquired with an Advance PET scanner (General Electrics Medical Systems, Wukesha, WI, U.S.A.) run in 3D mode. The transaxial resolution of this scanner is 5.5 mm full width at half-maximum (FWHM), and the axial resolution is 6.2 mm FWHM. In order to correct for tissue attenuation of photons a transmission scan of 5-min duration using two 400 MBq $^{68}$Ge pin sources was recorded prior to radiotracer injection. Then, enantiomerically pure *R*-[$^{11}$C]verapamil (368 $\pm$ 9 MBq, 10–20 nmoles), which had been synthesized from *R*-norverapamil (ABX advanced biochemical compounds, Radeberg, Germany) and [$^{11}$C]methyl triflate as described

**TABLE 1.** *Clinical, EEG, and ABCB1 genotype data of seven patients with refractory temporal lobe epilepsy*

| Patient | Age (years/sex) | Age (years) at onset of epilepsy | CPS/years | Interval last CPS to PET (days) | Medication (dose: mg/day) | Interval last medication intake to PET (h) | EEG (interictal) | EEG (ictal) | MRI | *ABCB1* haplotype (exon 12–21-26) |
|---|---|---|---|---|---|---|---|---|---|---|
| 1 | 37/M | 3 | 12 | 7 | LEV (1000), LTG (400) | 11 | Only few spikes RT | RT | R HA | TTT/TTT TTT/TTT |
| 2 | 50/M | 11 | 36 | 15 | OXC (1800) | 10 | LT | LT | L HA | CGT/TTT |
| 3 | 54/F | 3 | 12 | 17 | CBZ (750) | 11 | BT | LT | L HA | CGC/TTT |
| 4 | 52/F | 34 | 144 | 1 | LEV (3000), VPA (2000) | 11 (LEV) 7 (VPA) | RT | RT | Normal | CGC/CTT |
| 5 | 33/M | 20 | 70 | 6 | LEV (2000), OXC (2100) | 10 | BT | Independent LT and RT ict. EEG patterns | R HA | TTT/TTT |
| 6 | 50/M | 36 | 360 | 4 | PHT (300), LTG (400) | 4 | LT | LT | L HA | CGC/CGC |
| 7 | 44/M | 6 | 48 | 0 | LEV (3000), CBZ (1200) | 6 (LEV), 10 (CBZ) | RT | RT | R HA | CGC/TTT |

M, male; F, female; CPS, complex partial seizures; LEV, levetiracetam; LTG, lamotrigin; OXC, oxcarbazepine; CBZ, carbamazepine; VPA, valproic acid; PHT, phenytoin; EEG, electroencephalography; R, right; L, left; T, temporal; BT, bitemporal; HA, hippocampal atrophy; T, thymine; C, cytosine; G, guanine.

earlier (Brunner et al., 2005) and which was dissolved in 10 ml of physiological saline/ethanol (9/1, v/v), was injected as an intravenous bolus over 10 s. Radioactivity in brain was measured during 59.8 min by employing a consecutive frame sequence of 1 × 15, 3 × 5, 3 × 10, 2 × 30, 3 × 60, 2 × 150, 2 × 300 and 4 × 600 s. During the first 3 min after radiotracer injection, 4-ml arterial blood samples (24 ± 6) were withdrawn manually from the radial artery as fast as possible, followed by 9-ml samples taken at 3.5, 5, 10, 20, 30, 40, and 60 min after radiotracer injection. Radioactivity in whole blood and plasma was measured in a Packard Cobra II autogamma counter (Packard Instrument Company, Meriden, C.T., U.S.A.). The last seven plasma samples were analyzed for radiolabeled metabolites of *R*-[$^{11}$C]verapamil by employing a previously described solid-phase extraction procedure (Luurtsema et al., 2005). In this assay, total plasma radioactivity was corrected for polar radiolabeled metabolites (i.e., [$^{11}$C]formaldehyde and related species), which are generated by *N*-demethylation of *R*-[$^{11}$C]verapamil. The fraction containing unchanged *R*-[$^{11}$C]verapamil and its lipophilic radiolabeled metabolites (i.e., the *N*-dealkylation products $^{11}$C-labeled D-617 and D-717), which are known substrates for P-gp (Pauli-Magnus et al., 2000), was used to generate a partially metabolite-corrected arterial input function (Lubberink et al., 2006). For the 10, 20, 30, 40, and 60 min plasma sample the percentage of lipophilic radiolabeled metabolites of *R*-[$^{11}$C]verapamil was determined by injecting the eluate obtained from the solid-phase extraction assay (Luurtsema et al., 2005) into a high-performance liquid chromatography (HPLC) system. A Chromolith Performance RP-18e 100–4.6 mm HPLC column (Merck KGaA, Germany) was used, which was eluted isocratically with a 63/26/11 (v/v/v) mixture of 25 mM aqueous phosphate buffer (pH 7.0)/acetonitrile/methanol at a flow rate of 5 ml/min (injected volume: 2 ml). On this system unchanged *R*-[$^{11}$C]verapamil eluted with a retention time of 5–6 min and the radiolabeled metabolites eluted with the void volume.

All *R*-[$^{11}$C]verapamil PET scans were performed in the evening at 17:00–19:00 h, which was 10–11 h (patients 1, 2, 3, and 5) or 4–7 h (patients 4, 6, and 7) after intake of the last antiepileptic medication (Table 1). Patient 7 experienced a partial seizure during the PET scan (at 21 min after tracer injection) but completed the remainder of the PET examination.

### PET data processing

Reconstruction of the PET data was performed by means of iterative reconstruction using the ordered subsets-expectation maximization method with 28 subsets and two iterations. The loop filter (Gaussian) was set to a full-width at half-maximum (FWHM) of 4.3 mm, and a postfiltering algorithm of 6.0 mm FWHM was applied. Attenuation correction was performed using the manufacturer's segmentation algorithm for transmission data.

### Magnetic resonance imaging preprocessing

For volume of interest (VOI) definition, we used T1-weighted magnetic resonance imaging (MRI) scans of the brain acquired within 2 years prior to PET. The MRIs were simultaneously nonuniformity corrected and segmented into tissue classes using Statistical Parametric Mapping software (SPM5, Wellcome Department of Imaging Neuroscience, UCL, London, U.K.) (Ashburner and Friston, 2005). The process also yields spatial transformation information from the native MRI space into the Montreal Neurological Institute/International Consortsium for Brain Mapping standard stereotaxic space derived from 152 normal controls (MNI/ICBM152). This information

was used to spatially transform an updated version of a frequency-based anatomical atlas in MNI/ICBM space (Hammers et al., 2003) into native MRI space. The atlas was then thresholded with the MRI's grey matter tissue class thresholded at 50% probability.

### Derivation of regional PET data

The dynamic decay-corrected PET scans were coregistered onto the $T_1$-weighted MRIs using a normalized mutual information algorithm implemented in SPM5. For PET data analysis eight different temporal lobe VOIs (hippocampus, parahippocampal and ambient gyrus (PAHG), amygdala, medial and lateral anterior temporal lobe, lateral occipitotemporal (fusiform) gyrus, superior temporal gyrus, and middle together with inferior temporal gyrus), and one VOI in the parietal lobe (superior parietal gyrus) were outlined on MRI (Fig. 1) and sampled on the dynamic coregistered PET using Analyze AVW 7.0 software (Biomedical Imaging Resource, Mayo Foundation, Rochester, MN, U.S.A.) (Robb, 2001). In addition, the choroid plexus was drawn directly on the coregistered PET and sampled.

### Kinetic modeling of R-[11C]verapamil

A 1-tissue 2-parameter (1T2K) compartment model (Fig. 2) was fitted to the time-activity data of each brain-VOI (Lubberink et al., 2006). This model assumes that

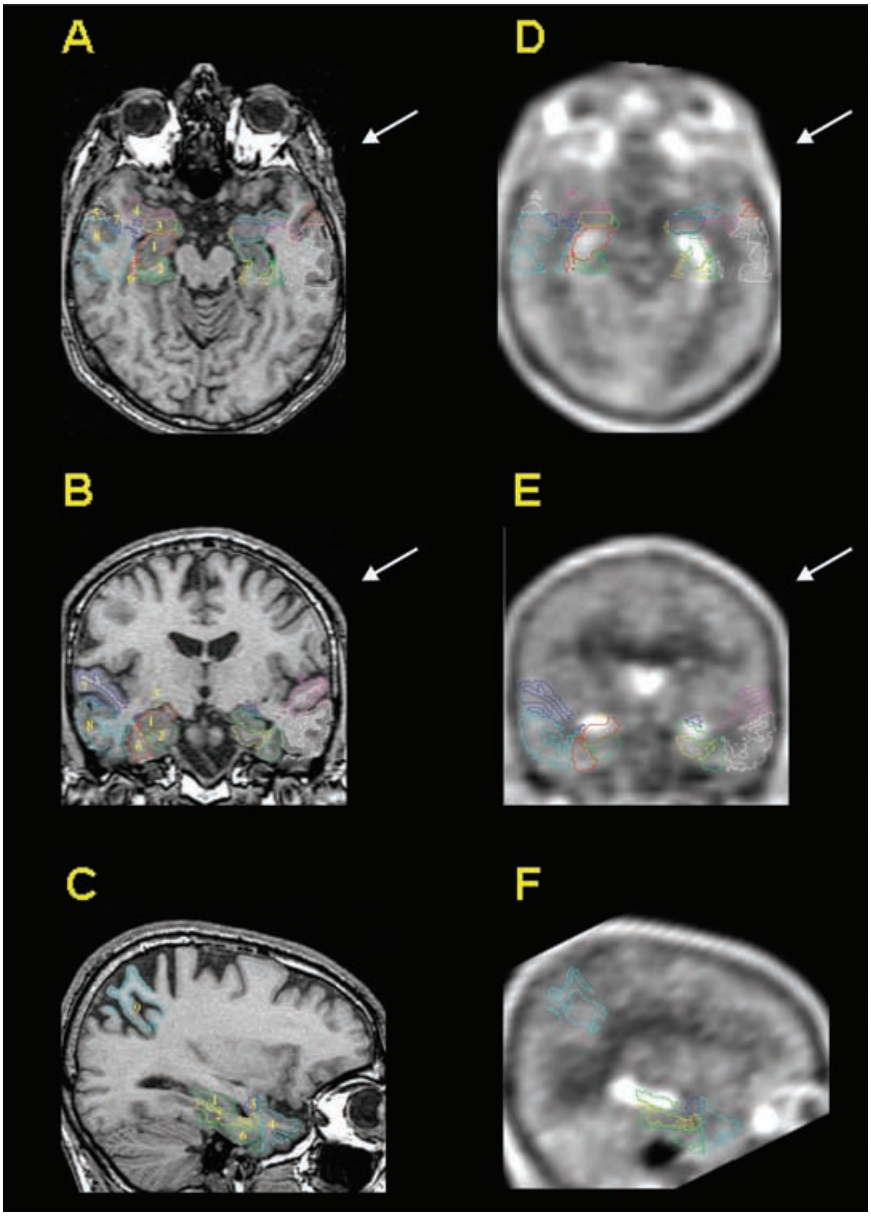


**FIG. 1.** $T_1$-weighted MR images (voxel size: 0.9 × 0.9 × 4 mm) showing VOIs **(A–C)** and PET summation images (20 frames) **(D–F)** showing the distribution of radioactivity after i.v. injection of *R*-[11C]verapamil into patient 6. The projections are from top to bottom: horizontal, coronal and sagittal (left hemisphere). The numbers in the MR images refer to the name of the regions: 1, hippocampus; 2, parahippocampal and ambient gyrus; 3, amygdala; 4, medial anterior temporal lobe; 5, lateral anterior temporal lobe; 6, lateral occipitotemporal (fusiform) gyrus; 7, superior temporal gyrus; 8, middle and inferior temporal gyrus; 9, superior parietal gyrus. The side of the seizure focus (left hemisphere) is indicated by an arrow. In the PET images, dark shades of grey represent low and light shades of grey high radioactivity concentrations.

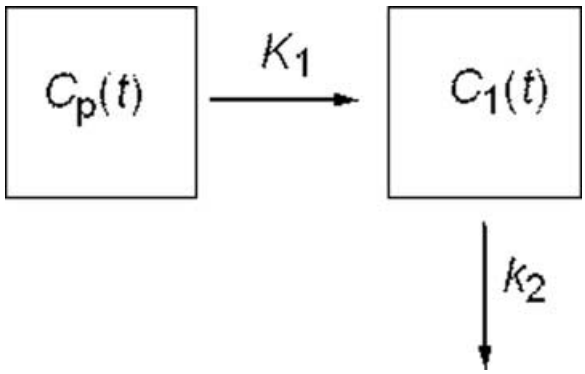


**FIG. 2.** Diagram of the 1-tissue 2-parameter (1T2K) compartment model used for the kinetic modeling of *R*-[$^{11}$C]verapamil PET data. $C_p(t)$ is the input function; $C_1(t)$ denotes the radioactivity concentration in brain tissue. $K_1$ (ml/ml/min) and $k_2$ (per min) are first-order rate constants. $K_1$ describes the influx of *R*-[$^{11}$C]verapamil and its lipophilic radiolabeled metabolites from plasma into brain tissue, whereas $k_2$ characterizes efflux of *R*-[$^{11}$C]verapamil and its lipophilic radiolabeled metabolites from brain tissue by P-gp transport and passive diffusion. The DV of *R*-[$^{11}$C]verapamil and its lipophilic radiolabeled metabolites (*DV*, ml/ml) is defined as $K_1/k_2$.

*R*-[$^{11}$C]verapamil and its lipophilic radiolabeled metabolites, which are also P-gp substrates, behave in a similar fashion and that their transport across the BBB can be described by simple linear (first-order) kinetics, that compartments are of homogeneous composition, and that the measured arterial plasma radioactivity concentrations can be used to approximate capillary concentrations within the respective VOIs. The 1T2K model is given by

$$\frac{dC_1(t)}{dt} = K_1 C_p(t) - k_2 C_1(t),$$

$$C_1(0) = 0$$

$C_p(t)$ is the input function to the 1T2K model; $C_p(t)$ was constructed by linear interpolation of the measured partially metabolite-corrected arterial plasma radioactivity data. $C_1(t)$ describes the radioactivity concentration in the brain tissue of the VOI. The first-order rate constants $K_1$ (ml·ml$^{-1}$·min$^{-1}$) and $k_2$ (min$^{-1}$) characterize the bidirectional transport of *R*-[$^{11}$C]verapamil and its lipophilic radiolabeled metabolites across the BBB. $K_2$ was considered as a measure of radioactivity elimination from brain by P-gp transport and passive diffusion (Fig. 2). The DV (*DV*, ml·ml$^{-1}$) is defined as $K_1/k_2$. The total radioactivity concentration $C(t)$ in the VOI was described by the equation

$$C(t) = (1 - V_b)C_1(t) + V_b C_b(t),$$

where $V_b$ is the vascular volume fraction of the VOI and $C_b(t)$ is the concentration-time course of radioactivity in whole blood. $C_b(t)$ was approximated by a constant fraction of $C_p(t)$; the ratio $C_b(t)/C_p(t)$ was determined by additional radioactivity measurements of arterial whole blood samples. The model equations were solved numerically using the *ode15s* solver of MATLAB (Mathworks, Natick, MA, U.S.A.). The kinetic parameters $K_1$, $k_2$, as well as the vascular volume fraction $V_b$ were estimated by fitting the 1T2K model to the measured PET data $C_{PET}(t_j)$ using the operational equation

$$\hat{C}_{PET}(t_j) = \frac{1}{te_j - ts_j} \int_{ts_j}^{te_j} C(t)dt,$$

where $ts_j$ and $te_j$ denote start and end time of the *j*th PET time frame and $t_j$ is its midpoint. Fits were performed by the method of weighted nonlinear least squares. In particular, the weighted residual sum of squares (WRSS),

$$\mathrm{WRSS} = \sum_{j=1}^{n} w_j \cdot \left[C_{PET}(t_j) - \hat{C}_{PET}(t_j)\right]^2,$$

was minimized using the *lsqnonlin* function of the *Optimization Toolbox* of MATLAB, where $n$ is the number of observed time-activity data points per VOI in each patient. The weighting factor $w_j$ was set to (Bertoldo et al., 2001)

$$w_j = \frac{te_j - ts_j}{\bar{C}_{PET}(t_j)},$$

where $\bar{C}_{PET}(t_j)$ are PET data not corrected for radioactive decay. Goodness-of-fit was assessed by visual inspection of observed and predicted TAC concentrations versus time, by the correlation between observed and predicted concentrations, by the randomness of the residuals (runs test), and by estimating parameter uncertainties (variances) from the inverse $\mathbf{M}^{-1}$ of the Fisher information matrix (Cobelli et al., 2000):

$$\mathrm{cov}(\mathbf{p}) = \frac{\mathrm{WRSS}(\mathbf{p})}{n - m} \cdot \mathbf{M}^{-1},$$

where $\mathbf{p}$ is the vector of the $m$ model parameters at the minimum of WRSS and where the variances of the parameter estimates are the diagonal elements of the covariance matrix cov($\mathbf{p}$).

In addition, in order to obtain a model-independent estimate of the DV, Logan graphical analysis (Logan et al., 1990) was applied to the PET and partially metabolite-corrected arterial plasma data using MATLAB. The slope *DV* of the linear part of the Logan plot was estimated by linear regression of the Logan variables. The linear regression was assessed by the magnitude of the squared linear correlation coefficient ($r^2$).

### Statistical analysis

Ipsilateral and contralateral model parameters ($K_1$, $k_2$, *DV*) in individual homologous brain VOIs were compared using the Wilcoxon matched pairs test employing commercially available software (STATISTICA Release 5.1, StatSoft, Inc., Tulsa, OK, U.S.A.). p-values $<0.05$

were considered significant. Ipsilateral versus contralateral parameter asymmetries ($K_1$, $k_2$, $DV$) were calculated as ([100/contralateral] × ipsilateral)-100.

## RESULTS

We scanned seven patients with drug-resistant unilateral TLE. The overall brain tissue uptake of *R*-[$^{11}$C]verapamil was low in contrast to the high radioactivity concentrations in the choroid plexus (Fig. 1). Radioactivity signal in hippocampus was contaminated by spill-in of radioactivity from the adjacent choroid plexus, so that this region could not be reliably used for further data analysis. The other temporal lobe regions, including parahippocampal and ambient gyrus (PAHG) and amygdala, appeared not to be affected by this artifact (Fig. 1).

Table 2 summarizes the influx rate constants $K_1$, the efflux rate constants $k_2$, and the DV of *R*-[$^{11}$C]verapamil in different homologous brain VOIs located ipsilateral and contralateral to the seizure focus. The mean interpatient coefficients of variation (CV) across all homologous brain VOIs were 21 ± 3% for $K_1$, 22 ± 4% for $k_2$ and 21 ± 3% for $DV$. The mean intrapatient CVs across all brain VOIs were 10 ± 1% for $K_1$, 13 ± 3% for $k_2$ and 8 ± 3% for $DV$. Compartmental model-derived $DV$ values were in good agreement with $DV$s estimated by Logan graphical analysis (data not shown). As compared to the other brain VOIs, $K_1$ and $DV$ values were about twofold higher in the choroid plexus; the contaminated hippocampal VOIs accordingly showed intermediate values (Table 2). In contrast to choroid plexus, radioactivity concentrations were in the ventricle system considerably lower than those in brain tissue (Fig. 1).

Fig. 3 shows $K_1$, $k_2$, and $DV$ asymmetries in different temporal and one extratemporal lobe VOI (superior parietal gyrus) expressed as percent difference between the ipsilateral versus the contralateral brain hemisphere. As compared to superior parietal gyrus, there were considerable $K_1$ and $k_2$ asymmetries for PAHG, amygdala, medial and lateral anterior temporal lobe and lateral occipitotemporal gyrus (Fig. 3A and 3B). The mean ipsilateral-to-contralateral differences in $K_1$ were +6.8% (range: −3.8% to +22.3%) for PAHG, +6.8% (range: −20.6% to +31.3%) for amygdala, +5.6% (range: −8.3% to +14.5%) for medial anterior temporal lobe, −2.1% (range: −20.7% to +16.8%) for lateral anterior temporal lobe, +2.5% (range: −5.9% to +12.1%) for lateral occipitotemporal gyrus and +0.9% (range: −3.7% to +4.5%) for superior parietal gyrus. For $k_2$, these differences were +10.0% (range: −2.3% to +43.9%) for PAHG, +8.7% (range: −18.0% to +38.9%) for amygdala, +8.4% (range: −14.5% to +31.0%) for medial anterior temporal lobe, +3.6% (range: −24.4% to +22.6%) for lateral anterior temporal lobe, +2.4% (range: −23.0% to +29.6%) for lateral occipitotemporal gyrus and +2.0% (range: −4.2% to +5.8%) for superior parietal gyrus.

In several cases, $k_2$ increases were more pronounced than $K_1$ increases resulting in ipsilateral decreased $DV$s of *R*-[$^{11}$C]verapamil (Fig. 3C). In five of seven patients (i.e., patient 2, 3, 5, 6, and 7) there were prominent (10%–26%) ipsilateral reductions of $DV$ in diverse temporal lobe regions. Fig. 4 shows time-activity curves of *R*-[$^{11}$C]verapamil in ipsi- and contralateral lateral anterior temporal lobe of patient 2 and PAHG of patient 5. For none of the examined brain regions, any of the differences in $K_1$, $k_2$, and $DV$ between the epileptogenic and the nonepileptogenic hemisphere reached statistical significance ($p > 0.05$, Wilcoxon matched pairs test). For PAHG, however, statistical comparison of ipsilateral and contralateral $k_2$ values gave a considerably lower p-value ($p = 0.091$) than for the other brain VOIs ($P > 0.3$).

In Table 3, the mean percentages of *R*-[$^{11}$C]verapamil and its radiolabeled metabolites in arterial plasma at different time points after tracer injection are summarized. At 60 min after injection, unchanged *R*-[$^{11}$C]verapamil represented 25.0 ± 6.3% of total radioactivity. The remainder of radioactivity was composed to about equal parts of lipophilic and polar radiolabeled metabolites of *R*-[$^{11}$C]verapamil.

All study participants were genotyped for *ABCB1* SNPs in exons 12 (C1236T), 21 (G2677T) and 26 (C3435T). The individual haplotypes are shown in Table 1. Mean $k_2$ values across all brain VOIs were 0.0348 ± 0.004 min$^{-1}$ for patient 6, a homozygous carrier of the CGC haplotype (CGC/CGC), and 0.0324 ± 0.004 min$^{-1}$ for patient 1 and 0.0341 ± 0.004 min$^{-1}$ for patient 5, who had both homozygous mutant haplotypes (TTT/TTT). Because of the low number of subjects in each group no statistical test was performed.

## DISCUSSION

In the present pilot study, the radiolabeled model P-gp substrate *R*-[$^{11}$C]verapamil and PET was used to assess P-gp functionality in the brains of patients with TLE, a form of focal epilepsy, which is often refractory to medical treatment. We analyzed different temporal lobe VOIs including hippocampus, parahippocampal, and ambient gyrus (PAHG) and amygdala, which are regions that are involved in seizure generation. Unfortunately, the most interesting epileptogenic brain region, i.e., hippocampus, could not be analyzed due to spill-in of radioactivity from the adjacent choroid plexus (Fig. 1). The high choroid plexus signal of *R*-[$^{11}$C]verapamil may be related to the expression of P-gp in the epithelium of the choroid plexus, resulting in active transport of P-gp substrates such as verapamil from blood into cerebral spinal fluid (Rao et al., 1999).

Model parameters from the side ipsilateral to the seizure focus were compared with respective parameters from the contralateral brain hemisphere in homologous VOIs (Fig. 3). In several temporal lobe VOIs that are adjacent to

**TABLE 2.** *Kinetic rate constants ($K_1$, $k_2$) and distribution volumes (DVs) of R-[$^{11}$C]verapamil in seven representative brain VOIs located ipsilateral and contralateral to the seizure focus and in choroid plexus. The estimated coefficient of variation in percent for each parameter is given in parentheses (see Methods section for further details)*

| Patient | $K_1$ (ml·ml$^{-1}$·min$^{-1}$); × $10^{-2}$ ipsilateral/contralateral | $k_2$ (min$^{-1}$); × $10^{-2}$ ipsilateral/contralateral | *DV* (ml·ml$^{-1}$) ipsilateral/contralateral | $K_1$ (ml·ml$^{-1}$·min$^{-1}$); × $10^{-2}$ ipsilateral/contralateral | $k_2$ (min$^{-1}$); × $10^{-2}$ ipsilateral/contralateral | *DV* (ml·ml$^{-1}$) ipsilateral/contralateral |
|---|---|---|---|---|---|---|
| | | *Hippocampus*[a] | | | *Parahippocampal + ambient gyrus* | |
| 1 | 3.75 (3.2)/4.46 (7.4) | 3.83 (4.5)/4.37 (7.6) | 0.98 (2.0)/1.02 (2.0) | 2.58 (4.5)/2.16 (3.3) | 3.47(6.2)/3.04 (5.1) | 0.74 (2.4)/0.71 (2.3) |
| 2 | 5.03 (5.7)/4.29 (4.5) | 4.76 (6.2)/4.81 (5.0) | 1.06 (1.9)/0.89 (1.3) | 3.40 (6.1)/3.28 (6.5) | 5.01 (6.6)/4.59 (7.3) | 0.68 (1.6)/0.72 (1.7) |
| 3 | 5.04 (2.7)/6.09 (2.3) | 3.45 (3.6)/4.13 (2.7) | 0.95 (1.5)/1.47 (1.0) | 3.75 (2.6)/3.90 (3.2) | 3.60 (3.8)/3.59 (5.0) | 1.04 (1.4)/1.09 (2.5) |
| 4 | 5.63 (2.3)/6.02 (3.3) | 3.71 (3.0)/3.54 (4.0) | 1.52 (1.2)/1.70 (1.4) | 3.77 (3.9)/3.77 (3.1) | 3.77 (6.1)/3.86 (4.9) | 1.00 (3.0)/0.98 (2.4) |
| 5 | 6.61 (3.0)/5.40 (5.1) | 5.19 (3.4)/3.91 (5.8) | 1.27 (1.2)/1.38 (1.9) | 4.00 (3.9)/3.27 (4.6) | 4.00 (4.9)/2.78 (7.7) | 1.00 (1.8)/1.18 (3.6) |
| 6 | 5.45 (4.3)/4.33 (2.3) | 4.65 (4.7)/4.43 (2.9) | 1.17 (1.5)/0.98 (1.1) | 2.86 (2.5)/2.72 (2.5) | 3.47 (3.5)/3.42 (3.5) | 0.82 (1.2)/0.80 (1.4) |
| 7 | 5.01 (4.6)/4.22 (5.0) | 4.09 (4.9)/3.07 (7.2) | 1.23 (1.8)/1.38 (3.0) | 2.86 (3.3)/2.83 (3.0) | 2.46 (6.4)/2.38 (6.3) | 1.16 (3.7)/1.19 (3.6) |
| | | *Amygdala* | | | *Medial anterior temporal lobe* | |
| 1 | 1.75 (6.9)/2.11 (11.4) | 2.60 (10.3)/3.17 (15.8) | 0.67 (4.3)/0.66 (6.4) | 1.96 (4.7)/1.77 (6.5) | 3.10 (6.2)/2.64 (8.6) | 0.63 (2.2)/0.67 (2.8) |
| 2 | 3.40 (9.7)/2.59 (8.2) | 5.86 (10.2)/4.22 (9.8) | 0.58 (2.6)/0.61 (2.9) | 2.88 (4.1)/3.14 (3.9) | 3.53 (5.6)/4.13 (4.8) | 0.82 (2.0)/0.76 (1.6) |
| 3 | 2.81 (3.8)/3.54 (6.1) | 3.72 (4.6)/3.84 (8.4) | 0.75 (1.5)/0.92 (3.4) | 3.24 (4.8)/2.99 (4.6) | 3.42 (6.6)/2.61 (6.6) | 0.95 (2.4)/1.15 (2.6) |
| 4 | 3.98 (2.7)/3.24 (2.9) | 3.59 (3.4)/2.95 (4.6) | 1.11 (1.1)/1.10 (2.0) | 3.58 (2.9)/3.43 (4.5) | 3.39 (4.1)/3.37 (6.8) | 1.05 (1.5)/1.02 (2.8) |
| 5 | 4.12 (8.0)/3.34 (5.2) | 4.14 (8.8)/3.36 (8.1) | 1.00 (2.4)/0.99 (3.4) | 3.38 (3.0)/3.03 (5.6) | 3.06 (4.6)/2.66 (7.6) | 1.10 (2.0)/1.14 (2.7) |
| 6 | 2.45 (2.1)/2.54 (3.1) | 2.92 (3.5)/2.98 (4.6) | 0.84 (1.7)/0.85 (1.9) | 2.57 (3.3)/2.62 (3.4) | 3.07 (4.6)/3.18 (4.7) | 0.84 (1.7)/0.83 (1.8) |
| 7 | 2.58 (3.8)/2.31 (9.3) | 2.12 (7.1)/2.11 (16.9) | 1.22 (3.8)/1.10 (8.3) | 2.53 (2.4)/2.21 (5.9) | 1.99 (4.7)/1.77 (12.1) | 1.27 (2.5)/1.25 (6.6) |
| | | *Lateral anterior temporal lobe* | | | *Lateral occipitotemporal gyrus* | |
| 1 | 1.84 (4.1)/2.32 (3.6) | 2.76 (6.3)/3.65 (4.4) | 0.67 (2.7)/0.63 (1.4) | 2.49 (5.3)/2.26 (4.5) | 3.92 (6.0)/3.35 (5.1) | 0.64 (1.7)/0.67 (1.3) |
| 2 | 3.01 (6.5)/3.55 (5.5) | 4.67 (7.4)/4.13 (6.3) | 0.64 (1.9)/0.86 (1.6) | 3.13 (5.1)/3.15 (4.0) | 3.58 (6.9)/4.65 (4.5) | 0.87 (2.5)/0.68 (1.2) |
| 3 | 3.71 (3.9)/3.68 (7.6) | 3.82 (4.9)/3.57 (8.2) | 0.97 (1.6)/1.03 (1.5) | 3.73 (4.6)/3.86 (3.1) | 3.40 (5.8)/3.50 (4.6) | 1.10 (1.8)/1.10 (2.0) |
| 4 | 4.58 (2.0)/4.56 (1.9) | 4.29 (2.3)/4.38 (2.4) | 1.07 (0.8)/1.04 (1.0) | 4.15 (2.8)/3.86 (2.3) | 3.93 (3.7)/3.84 (2.9) | 1.06 (1.4)/1.00 (1.0) |
| 5 | 3.83 (5.9)/3.28 (5.7) | 3.42 (8.1)/2.79 (8.4) | 1.12 (2.9)/1.18 (3.3) | 3.55 (2.5)/3.63 (3.6) | 3.14 (3.9)/3.50 (4.9) | 1.13 (1.8)/1.04 (2.0) |
| 6 | 2.82 (2.6)/2.89 (3.2) | 3.43 (3.9)/3.35 (4.6) | 0.82 (1.6)/0.86 (1.7) | 3.06 (3.0)/2.73 (4.5) | 3.90 (3.8)/3.01 (6.4) | 0.79 (1.3)/0.90 (2.5) |
| 7 | 2.78 (4.2)/2.63 (3.6) | 2.42 (6.1)/2.27 (5.7) | 1.15 (2.4)/1.16 (2.4) | 2.40 (4.7)/2.55 (4.1) | 1.93 (9.0)/1.85 (7.9) | 1.24 (4.8)/1.38 (4.1) |
| | | *Superior parietal gyrus* | | | *Choroid plexus*[b] | |
| 1 | 2.45 (2.7)/2.42 (4.6) | 3.17 (3.9)/3.31 (5.9) | 0.77 (1.7)/0.73 (1.9) | 6.18 (1.9) | 4.55 (2.3) | 1.36 (1.0) |
| 2 | 3.51 (3.6)/3.36 (3.6) | 5.29 (3.8)/5.00 (4.2) | 0.66 (0.9)/0.67 (1.3) | 5.60 (2.7) | 4.87 (3.0) | 1.15 (0.9) |
| 3 | 3.66 (2.7)/3.80 (5.8) | 3.83 (3.7)/3.95 (6.3) | 0.95 (1.5)/0.96 (1.7) | 7.35 (2.4) | 3.43 (3.1) | 2.14 (1.3) |
| 4 | 4.22 (3.5)/4.25 (3.0) | 4.54 (3.8)/4.44 (3.8) | 0.93 (1.1)/0.96 (1.3) | 7.57 (1.7) | 3.96 (2.1) | 1.91 (1.0) |
| 5 | 3.64 (6.4)/3.70 (5.2) | 3.77 (7.7)/3.61 (7.1) | 0.97 (2.3)/1.02 (2.8) | 7.28 (2.0) | 4.09 (2.3) | 1.78 (0.9) |
| 6 | 3.09 (2.6)/2.98 (3.0) | 3.83 (3.2)/3.72 (3.0) | 0.81 (1.0)/0.80 (1.1) | 6.36 (2.0) | 5.12 (2.2) | 1.24 (0.6) |
| 7 | 3.13 (5.4)/3.05 (6.3) | 2.93 (9.5)/2.77 (9.9) | 1.07 (4.5)/1.10 (4.3) | 5.54 (7.6) | 3.26 (9.5) | 1.70 (2.7) |

[a]Hippocampus signal was contaminated by spill-in from choroid plexus and values are just shown for illustrative purposes.
[b]Choroid plexus was manually defined.

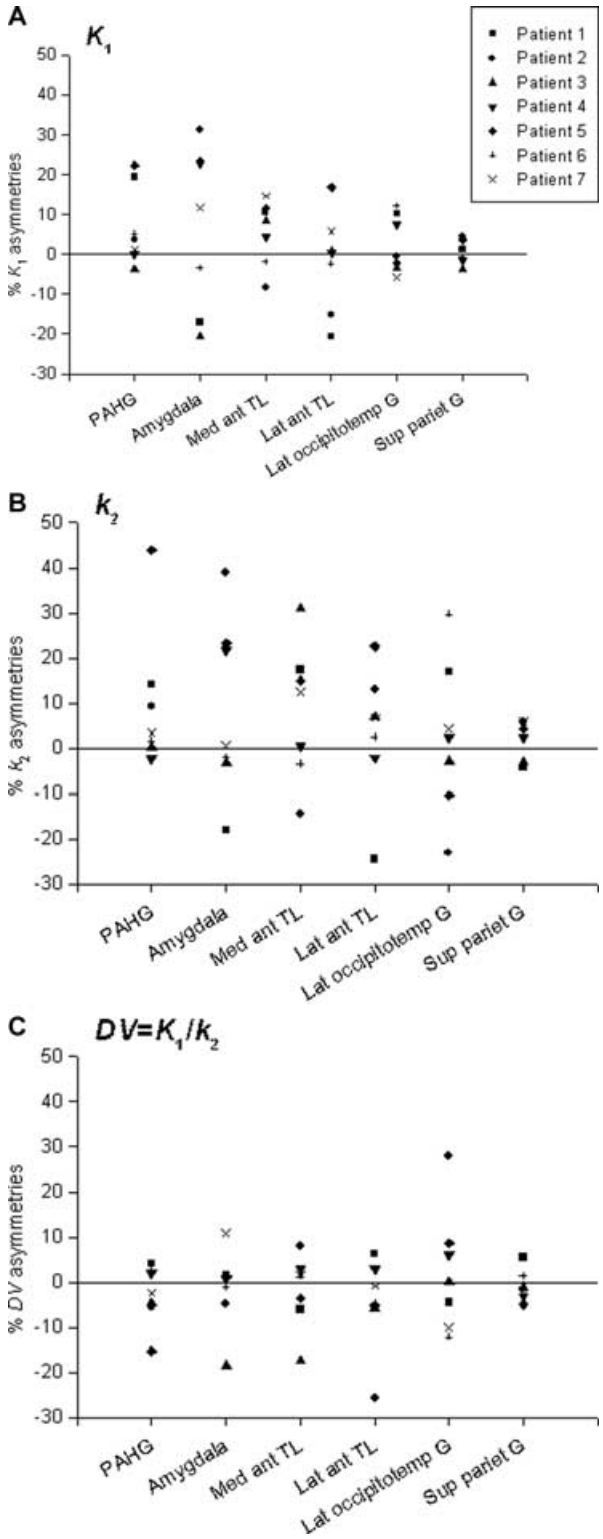


**FIG. 3.** Scatter plots showing percent ipsilateral vs. contralateral asymmetries for the influx rate constant $K_1$ **(A)**, the efflux rate constant $k_2$ **(B)** and the DV (i.e., $K_1/k_2$) **(C)** of *R*-[11C]verapamil in five different temporal lobe VOIs and the extratemporal control VOI (superior parietal gyrus) in seven patients with TLE. PAHG, parahippocampal and ambient gyrus; med, medial; ant, anterior; TL, temporal lobe; lat, lateral; occipitotemp, occipitotemporal; G, gyrus; sup, superior; pariet, parietal.

the hippocampus and that are implicated in seizure generation and propagation, we observed ipsilaterally increased influx and efflux rate constants of *R*-[11C]verapamil (Table 2, Fig. 3). These asymmetries were most prominent in PAHG, amygdala, and medial and lateral anterior temporal lobe. In several brain regions, ipsilateral $k_2$ increases were more pronounced than ipsilateral $K_1$

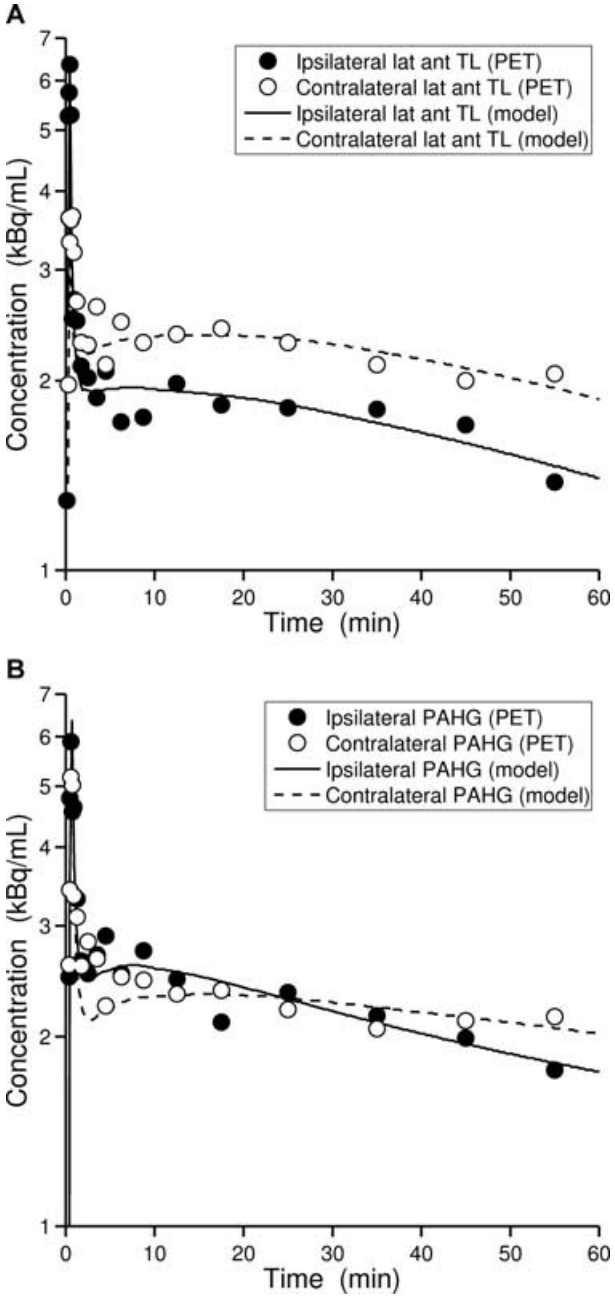


**FIG. 4.** *R*-[11C]verapamil time-activity curves and fits obtained from the 1-tissue 2-parameter compartment model in ipsi- and contralateral lateral anterior temporal lobe of patient 2 **(A)** and parahippocampal and ambient gyrus (PAHG) of patient 5 **(B)**. Note that the y-axis is in a logarithmic scale. The ipsilateral distribution volumes were reduced by 26% for patient 2 and by 15% for patient 5.

**TABLE 3.** *R-[$^{11}$C]verapamil and its radiolabeled metabolites in arterial plasma (% of total radioactivity, mean ± standard deviation) at different time points after intravenous injection of R-[$^{11}$C]verapamil into seven patients with refractory temporal lobe epilepsy*

| Time (min) | *R*-[$^{11}$C] verapamil | Lipophilic [$^{11}$C]metabolites | [$^{11}$C]Polar fraction |
|---|---|---|---|
| 3.6 ± 0.0[a] | 97.3 ± 2.1 | – | 2.7 ± 2.1 |
| 5.1 ± 0.1[a] | 91.7 ± 5.2 | – | 8.3 ± 5.2 |
| 10.3 ± 0.4 | 69.2 ± 13.1 | 14.6 ± 7.7 | 15.1 ± 5.8 |
| 20.1 ± 0.0 | 51.5 ± 11.0 | 22.9 ± 4.3 | 25.6 ± 7.1 |
| 30.3 ± 0.6 | 40.6 ± 7.6 | 31.5 ± 3.3 | 27.9 ± 3.0 |
| 40.3 ± 0.1 | 37.8 ± 10.6 | 32.2 ± 6.1 | 30.0 ± 7.6 |
| 60.3 ± 0.1 | 25.0 ± 6.3 | 35.9 ± 3.8 | 39.0 ± 7.9 |

[a]For the first two time points no HPLC was performed and the *R*-[$^{11}$C]verapamil fraction therefore also includes lipophilic [$^{11}$C]metabolites.

increases, which resulted in ipsilateral decreased *DV*s of *R*-[$^{11}$C]verapamil (Figs. 3C, 4). These differences did not reach statistical significance in the group, which might be explained by the fact that the observed effects were variable and not restricted to a single brain VOI but rather spread over different temporal lobe VOIs. Despite the lack of statistical significance, our findings are intriguing as they point to enhanced P-gp activity in epileptic brain regions, even though it cannot be excluded that similar parameter asymmetries would be present in temporal lobe regions of drug-responsive patients. Ipsilateral versus contralateral *DV* asymmetries were heterogeneous, with 10%–26% ipsilateral *DV* reductions observed in some regions for five of seven patients while only moderate *DV* reductions or even moderate *DV* increases were seen in other regions. It is tempting to speculate that the heterogeneity of the data reflects different levels of temporal lobe P-gp activity in different individuals. Our data are in line with the concept that the mechanisms of pharmacoresistance are multifactorial and that P-gp-mediated efflux is only in some refractory patients a descriptor of multidrug resistance (Löscher, 2005). In contrast to temporal lobe VOIs, parameter asymmetries were minimal in a brain region located outside the temporal lobe (superior parietal gyrus, Fig. 3), which supports the notion that the observed asymmetries were indeed unique to epileptic brain regions. In addition, earlier data acquired with racemic [$^{11}$C]verapamil in healthy volunteers had shown no comparable side-to-side differences in regional [$^{11}$C]verapamil brain tissue concentrations and efflux (Brunner et al., 2005).

A surprising finding of this study are the ipsilaterally increased influx rate constants $K_1$ of *R*-[$^{11}$C]verapamil in several temporal lobe VOIs (Fig. 3A). It has recently been suggested that not only $k_2$ but also $K_1$ of [$^{11}$C]verapamil should be affected by P-gp function, in that increased P-gp activity leads to decreased substrate influx $K_1$ (influx hindrance) (Ikoma et al., 2006; Sasongko et al., 2005). The ipsilateral $K_1$ increases observed in this study might be related to regionally enhanced blood flow and/or tissue extraction of *R*-[$^{11}$C]verapamil and might have masked possible $K_1$ decreases caused by the "gatekeeper" function of P-gp (Siarheyeva et al., 2006; Syvänen et al., 2006b).

An important issue that has to be considered in this study is the fact that all our patients were being treated with AEDs. Even though it is at present not entirely clear which AEDs are transported to what extent by P-gp in humans (Owen et al., 2001; Potschka et al., 2001), it can be expected that in at least some of the patients of this study the antiepileptic medication might have competed with *R*-[$^{11}$C]verapamil for P-gp transport, which could have accounted for the variable and in some cases modest *DV* decreases of *R*-[$^{11}$C]verapamil in epileptic brain tissue. In order to address the issue of possible P-gp occupancy by AEDs in the future, repeated *R*-[$^{11}$C]verapamil PET scans in patients during AED treatment and during treatment discontinuation (e.g., during epilepsy monitoring) would be highly interesting.

Polymorphisms in the *ABCB1* gene might have contributed to the observed interpatient variability of our PET data as these have been associated with changes in P-gp expression and function (Hoffmeyer et al., 2000). A recent study has found an association of the *ABCB1* exon 26 C3435T polymorphism with multidrug resistance in epilepsy patients (Siddiqui et al., 2003). In another study a correlation has been found between *ABCB1* SNPs in exons 12 (C1236T), 21 (G2677T) and 26 (C3435T) and drug resistance in patients with TLE, with an increased risk of drug resistance for homozygous carriers of the CGC haplotype (1236C, 2677G, 3435C) (Zimprich et al., 2004). Other studies, however, have failed to replicate these findings (Sills et al., 2005; Tan et al., 2004). In the present study all study participants were genotyped for *ABCB1* SNPs in exons 12, 21 and 26 (Table 1). According to the present pilot data from a small sample size of epilepsy patients no apparent relationship between the *ABCB1* genotype and the *R*-[$^{11}$C]verapamil efflux rate constant $k_2$ could be described. However, more studies in larger groups of epilepsy patients are needed to determine the true impact of *ABCB1* haplotypes on P-gp function at the BBB.

In summary, despite the lack of statistical significance it cannot be excluded from our pilot data that regionally enhanced P-gp activity might be involved in drug resistance in at least some of the patients included in this study. These findings might have important therapeutic implications as they support the development of P-gp inhibitors as antiepileptic comedication (Sisodiya and Bates, 2006). Several new third-generation P-gp inhibitors, such as tariquidar (XR-9576), are currently in clinical development (Szakacs et al., 2006). Initially developed to overcome multidrug resistance in oncology, none of these substances has been tested in clinical trials in epilepsy

patients (Bates et al., 2002; Sisodiya and Bates, 2006). In future clinical trials with P-gp modulators, PET scans using *R*-[$^{11}$C]verapamil might be useful to identify patients with pronounced cerebral P-gp activity, which would most likely benefit from P-gp modulation. Our data, however, indicate that TLE is probably not the best suited epilepsy form for PET studies with *R*-[$^{11}$C]verapamil due to pronounced partial volume effects in the hippocampus. Other patient groups, such as patients with focal cortical dysplasia, may possibly be better suited for direct analysis of epileptogenic brain regions to further elucidate the role of P-gp in treatment-refractory epilepsy.

**Acknowledgments:** This study could not have been completed without the excellent technical support of Rainer Bartosch and Ingrid Leitinger from the Department of Nuclear Medicine, and research nurse Edith Lackner from the Department of Clinical Pharmacology. David Elmenhorst (Research Centre Jülich, Germany) is gratefully acknowledged for help and advice with arterial blood sampling. We further wish to thank Mark Lubberink and Adriaan Lammertsma from the VU University Medical Center (Amsterdam, The Netherlands) for help with setting up the *R*-[$^{11}$C]verapamil PET procedure in our laboratory. Federico Türkheimer from the MRC Clinical Sciences Centre and Division of Neuroscience, and Marie-Claude Asselin, Rainer Hinz and Julian Matthews from the Wolfson Molecular Imaging Centre (Manchester, United Kingdom), and Friederike Neumann from the Department of Medical Computer Sciences gave very valuable advice regarding PET data.

## REFERENCES

Aronica E, Gorter JA, Ramkema M, Redeker S, Ozbas-Gerceker F, van Vliet EA, Scheffer GL, Scheper RJ, Van Der Valk P, Baayen JC, Troost D. (2004) Expression and cellular distribution of multidrug resistance-related proteins in the hippocampus of patients with mesial temporal lobe epilepsy. *Epilepsia* 45:441–451.

Ashburner J, Friston KJ. (2005) Unified segmentation. *Neuroimage* 26:839–851.

Baltes S, Potschka H, Luna Tortos C, Fedrowitz M, Löscher W. (2006) Valproic acid is not a substrate for P-glycoprotein or multidrug resistance proteins MRP1 and MRP2 in a number of in vitro and in vivo transport assays. *Journal of Pharmacological Experiment and Therory*: doi:10.1124/jpet.106.102491.

Bates SF, Chen C, Robey R, Kang M, Figg WD, Fojo T. (2002) Reversal of multidrug resistance: lessons from clinical oncology. *Novartis Foundation Symposium* 243:83–96; discussion 96–102, 180–105.

Bertoldo A, Peltoniemi P, Oikonen V, Knuuti J, Nuutila P, Cobelli C. (2001) Kinetic modeling of [(18)F]FDG in skeletal muscle by PET: a four-compartment five-rate-constant model. *American Journal of Physiology, Endocrinology, and Metabolism* 281:E524–536.

Bourgeois BFD (2001) General concepts of medical intractability. In Lüders HO, Comair YG (Eds) *Epilepsy surgery*. Lippincott Williams & Wilkins, Philadelphia, pp. 63–68.

Brunner M, Langer O, Sunder-Plassmann R, Dobrozemsky G, Müller U, Wadsak W, Krcal A, Karch R, Mannhalter C, Dudczak R, Kletter K, Steiner I, Baumgartner C, Müller M. (2005) Influence of functional haplotypes in the drug transporter gene ABCB1 on central nervous system drug distribution in humans. *Clinical Pharmacology and Therapeutics* 78:182–190.

Cobelli C, Foster D, Toffolo G (2000) *Tracer kinetics in biomedical research: from data to model*. Kluwer Academic/Plenum, New York.

Dombrowski SM, Desai SY, Marroni M, Cucullo L, Goodrich K, Bingaman W, Mayberg MR, Bengez L, Janigro D. (2001) Overexpression of multiple drug resistance genes in endothelial cells from patients with refractory epilepsy. *Epilepsia* 42:1501–1506.

Elsinga PH, Franssen EJ, Hendrikse NH, Fluks L, Weemaes AM, Van Der Graaf WT, de Vries EG, Visser GM, Vaalburg W. (1996) Carbon-11-labeled daunorubicin and verapamil for probing P-glycoprotein in tumors with PET. *Journal of Nuclear Medicine* 37:1571–1575.

Franssen EJ, Luurtsema G, Lammertsma AA. (2006) Imaging P-glycoprotein at the human blood-brain barrier. *Clinical Pharmacology and Therapy* 80:302–303; author reply 303–304.

Hammers A, Allom R, Koepp MJ, Free SL, Myers R, Lemieux L, Mitchell TN, Brooks DJ, Duncan JS. (2003) Three-dimensional maximum probability atlas of the human brain, with particular reference to the temporal lobe. *Human Brain Mapping* 19:224–247.

Hendrikse NH, Schinkel AH, de Vries EG, Fluks E, Van Der Graaf WT, Willemsen AT, Vaalburg W, Franssen EJ. (1998) Complete in vivo reversal of P-glycoprotein pump function in the blood-brain barrier visualized with positron emission tomography. *British Journal of Pharmacology* 124:1413–1418.

Hoffmeyer S, Burk O, von Richter O, Arnold HP, Brockmoller J, Johne A, Cascorbi I, Gerloff T, Roots I, Eichelbaum M, Brinkmann U. (2000) Functional polymorphisms of the human multidrug-resistance gene: multiple sequence variations and correlation of one allele with P-glycoprotein expression and activity in vivo. *Proceedings of the National Academy of Sciences of USA* 97:3473–3478.

Ikoma Y, Takano A, Ito H, Kusuhara H, Sugiyama Y, Arakawa R, Fukumura T, Nakao R, Suzuki K, Suhara T. (2006) Quantitative analysis of 11C-verapamil transfer at the human blood-brain barrier for evaluation of P-glycoprotein function. *Journal of Nuclear Medicine* 47:1531–1537.

Kortekaas R, Leenders KL, van Oostrom JC, Vaalburg W, Bart J, Willemsen AT, Hendrikse NH. (2005) Blood-brain barrier dysfunction in parkinsonian midbrain in vivo. *Annals of Neurology* 57:176–179.

Lee YJ, Maeda J, Kusuhara H, Okauchi T, Inaji M, Nagai Y, Obayashi S, Nakao R, Suzuki K, Sugiyama Y, Suhara T. (2006) In vivo evaluation of P-glycoprotein function at the blood-brain barrier in nonhuman primates using [11C]verapamil. *Journal Pharmacology and Experimental Therapeutics* 316:647–653.

Logan J, Fowler JS, Volkow ND, Wolf AP, Dewey SL, Schlyer DJ, MacGregor RR, Hitzemann R, Bendriem B, Gatley SJ, et al. (1990) Graphical analysis of reversible radioligand binding from time-activity measurements applied to [N-11C-methyl]-(-)-cocaine PET studies in human subjects. *Journal of Cerebral Blood Flow and Metabolism* 10:740–747.

Löscher W. (2005) How to explain multidrug resistance in epilepsy? *Epilepsy Current* 5:107–112.

Löscher W, Potschka H. (2002) Role of multidrug transporters in pharmacoresistance to antiepileptic drugs. *Journal of Pharmacology and Experimental Therapeutics* 301:7–14.

Löscher W, Potschka H. (2005) Blood-brain barrier active efflux transporters: ATP-binding cassette gene family. *NeuroRx* 2:86–98.

Lubberink M, Luurtsema G, van Berckel BN, Boellaard R, Toornvliet R, Windhorst AD, Franssen EJ, Lammertsma AA. (2006) Evaluation of tracer kinetic models for quantification of P-glycoprotein function using (R)-[(11)C]verapamil and PET. *Journal of Cerebral Blood Flow Metabolism*: doi: 10.1038/sj.jcbfm.9600349.

Luurtsema G, Molthoff CF, Schuit RC, Windhorst AD, Lammertsma AA, Franssen EJ. (2005) Evaluation of (R)-[11C]verapamil as PET tracer of P-glycoprotein function in the blood-brain barrier: kinetics and metabolism in the rat. *Nuclear Medicine and Biology* 32:87–93.

Owen A, Pirmohamed M, Tettey JN, Morgan P, Chadwick D, Park BK. (2001) Carbamazepine is not a substrate for P-glycoprotein. *British Journal of Clinical Pharmacology* 51:345–349.

Pauli-Magnus C, von Richter O, Burk O, Ziegler A, Mettang T, Eichelbaum M, Fromm MF. (2000) Characterization of the major metabolites of verapamil as substrates and inhibitors of P-glycoprotein. *Journal of Pharmacology and Experimental Therapeutics* 293:376–382.

Potschka H, Löscher W. (2001) In vivo evidence for P-glycoprotein-mediated transport of phenytoin at the blood-brain barrier of rats. *Epilepsia* 42:1231–1240.

Potschka H, Fedrowitz M, Löscher W. (2001) P-glycoprotein and multidrug resistance-associated protein are involved in the regulation of extracellular levels of the major antiepileptic drug carbamazepine in the brain. *Neuroreport* 12:3557–3560.

Potschka H, Fedrowitz M, Löscher W. (2003) Multidrug resistance protein MRP2 contributes to blood-brain barrier function and restricts

antiepileptic drug activity. *Journal of Pharmacology and Experimental Therapeutics* 306:124–131.

Potschka H, Baltes S, Löscher W. (2004) Inhibition of multidrug transporters by verapamil or probenecid does not alter blood-brain barrier penetration of levetiracetam in rats. *Epilepsy Research* 58: 85–91.

Rambeck B, Jurgens UH, May TW, Pannek HW, Behne F, Ebner A, Gorji A, Straub H, Speckmann EJ, Pohlmann-Eden B, Löscher W. (2006) Comparison of brain extracellular fluid, brain tissue, cerebrospinal fluid, and serum concentrations of antiepileptic drugs measured intraoperatively in patients with intractable epilepsy. *Epilepsia* 47:681–694.

Rao VV, Dahlheimer JL, Bardgett ME, Snyder AZ, Finch RA, Sartorelli AC, Piwnica-Worms D. (1999) Choroid plexus epithelial expression of MDR1 P glycoprotein and multidrug resistance-associated protein contribute to the blood-cerebrospinal-fluid drug-permeability barrier. *Proceedings of the National Academy of Sciences of USA* 96:3900–3905.

Remy S, Beck H. (2006) Molecular and cellular mechanisms of pharmacoresistance in epilepsy. *Brain* 129:18–35.

Robb RA. (2001) The biomedical imaging resource at Mayo Clinic. *IEEE Transactions on Medical Imaging* 20:854–867.

Sasongko L, Link JM, Muzi M, Mankoff DA, Yang X, Collier AC, Shoner SC, Unadkat JD. (2005) Imaging P-glycoprotein transport activity at the human blood-brain barrier with positron emission tomography. *Clinical Pharmacology and Therapeutics* 77:503–514.

Siarheyeva A, Lopez JJ, Glaubitz C. (2006) Localization of multidrug transporter substrates within model membranes. *Biochemistry* 45:6203–6211.

Siddiqui A, Kerb R, Weale ME, Brinkmann U, Smith A, Goldstein DB, Wood NW, Sisodiya SM. (2003) Association of multidrug resistance in epilepsy with a polymorphism in the drug-transporter gene ABCB1. *New England Journal of Medicine* 348:1442–1448.

Sills GJ, Mohanraj R, Butler E, McCrindle S, Collier L, Wilson EA, Brodie MJ. (2005) Lack of association between the C3435T polymorphism in the human multidrug resistance (MDR1) gene and response to antiepileptic drug treatment. *Epilepsia* 46:643–647.

Sisodiya SM, Bates SE. (2006) Treatment of drug resistance in epilepsy: one step at a time. *Lancet Neurology* 5:380–381.

Sisodiya SM, Heffernan J, Squier MV. (1999) Over-expression of P-glycoprotein in malformations of cortical development. *Neuroreport* 10:3437–3441.

Sunder-Plassmann R, Rieger S, Endler G, Brunner M, Müller M, Mannhalter C. (2005) Simultaneous analysis of MDR1 C3435T, G2677T/A, and C1236T genotypes by multiplexed mutagenically separated PCR. *Clinical Chemistry and Laboratory Medicine* 43:192–194.

Syvänen S, Blomquist G, Sprycha M, Urban Hoglund A, Roman M, Eriksson O, Hammarlund-Udenaes M, Långström B, Bergström M. (2006a) Duration and degree of cyclosporin induced P-glycoprotein inhibition in the rat blood-brain barrier can be studied with PET. *Neuroimage* 32:1134–1141.

Syvänen S, Xie R, Sahin S, Hammarlund-Udenaes M. (2006b) Pharmacokinetic consequences of active drug efflux at the blood–brain barrier. *Pharmaceutical Research* 23:705–717.

Szakacs G, Paterson JK, Ludwig JA, Booth-Genthe C, Gottesman MM. (2006) Targeting multidrug resistance in cancer. *Nat Rev Drug Discov* 5:219–234.

Tan NC, Heron SE, Scheffer IE, Pelekanos JT, McMahon JM, Vears DF, Mulley JC, Berkovic SF. (2004) Failure to confirm association of a polymorphism in ABCB1 with multidrug-resistant epilepsy. *Neurology* 63:1090–1092.

Tishler DM, Weinberg KI, Hinton DR, Barbaro N, Annett GM, Raffel C. (1995) MDR1 gene expression in brain of patients with medically intractable epilepsy. *Epilepsia* 36:1–6.

Toornvliet R, van Berckel BN, Luurtsema G, Lubberink M, Geldof AA, Bosch TM, Oerlemans R, Lammertsma AA, Franssen EJ. (2006) Effect of age on functional P-glycoprotein in the blood-brain barrier measured by use of (R)-[(11)C]verapamil and positron emission tomography. *Clinical Pharmacology and Therapeutics* 79:540–548.

Zimprich F, Sunder-Plassmann R, Stogmann E, Gleiss A, Dal-Bianco A, Zimprich A, Plumer S, Baumgartner C, Mannhalter C. (2004) Association of an ABCB1 gene haplotype with pharmacoresistance in temporal lobe epilepsy. *Neurology* 63:1087–1089.